

# Modelling airborne transmission of SARS-CoV-2 at a local scale

Simon Rahn\* and Marion Gödel†

Munich University of Applied Sciences HM, Department of Computer Science and Mathematics, 80335 Munich, Germany and  
Technical University of Munich, Department of Informatics, 85748 Garching, Germany

Gerta Köster‡

Munich University of Applied Sciences HM, Department of Computer Science and Mathematics, 80335 Munich, Germany

Gesine Hofinger§

Team HF, Hofinger, Künzer & Mähler PartG, 71634 Ludwigsburg, Germany

(Dated: 17th November 2021)

The coronavirus disease (COVID-19) pandemic has changed our lives and still poses a challenge to science. Numerous studies have contributed to a better understanding of the pandemic. In particular, inhalation of aerosolised pathogens has been identified as essential for transmission. This information is crucial to slow the spread, but the individual likelihood of becoming infected in everyday situations remains uncertain. Mathematical models help estimate such risks. In this study, we propose how to model airborne transmission of SARS-CoV-2 at a local scale. In this regard, we combine microscopic crowd simulation with a new model for disease transmission. Inspired by compartmental models, we describe agents' health status as susceptible, exposed, infectious or recovered. Infectious agents exhale pathogens bound to persistent aerosols, whereas susceptible agents absorb pathogens when moving through an aerosol cloud left by the infectious agent. The transmission depends on the pathogen load of the aerosol cloud, which changes over time. We propose a 'high risk' benchmark scenario to distinguish critical from non-critical situations. Simulating indoor situations show that the new model is suitable to evaluate the risk of exposure qualitatively and, thus, enables scientists or even decision-makers to better assess the spread of COVID-19 and similar diseases.

**Keywords:** agent-based modelling, microscopic crowd simulation, airborne transmission, aerosol, pathogen, SARS-CoV-2

## I. INTRODUCTION

The outbreak of coronavirus disease (COVID-19) started at the end of 2019. Within months, it spread around the world and, ultimately, the World Health Organization [1] characterised COVID-19 as a pandemic on 11 March 2020. It has affected many aspects of our daily lives. Therefore, scientists from various disciplines have attempted to answer urgent questions about the coronavirus and how it spreads.

From virology, we know that COVID-19 is caused by the severe acute respiratory syndrome coronavirus type 2 (SARS-CoV-2). It is predominantly transmitted via respiratory fluids [2, 3]. This refers to both airborne and droplet transmission. However, there is no clear line between smaller, airborne droplets and larger ones [4]. In this work, we focus on particles that remain airborne for at least a few minutes. We refer to these particles suspended in air *aerosol clouds*.

Modelling plays an important role in epidemiology. Computer simulations help better understand the dynamics of a pandemic when ethical concerns prohibit experimental studies. In the following, we discuss several

approaches whose scope ranges from large to small populations.

In their compartmental SIR model, Kermack and McKendrick [5] describe the course of an epidemic, more precisely, the number of susceptible (S), infectious (I) and removed (R) individuals among a population, with ordinary differential equations. This model was modified, e.g. by adding an exposed state (SEIR) to simulate the latent period or by accounting for possible reinfection after temporal immunity (SIRS). The deterministic approach approximates a stochastic process of contact networks and, thus, is only valid for large populations.

In contrast, agent-based models capture the spread of diseases among smaller populations. All virtual persons, the so-called agents, possess individual properties, such as their health condition. The transition from one status to another, e.g. from susceptible to infected, depends on predefined rules. These rules are often based on mutual distances. For example, agents close to an infectious agent become infected after a certain time (see [6–9]). Ronchi and Lovreglio [10] expand the concept of proximity to further contact types, e.g. physical contact, proximity within a certain radius and occupancy of the same room or building. The overall time spent in contact determines the risk of exposure. Generally, agent-based models focus on contact time and proximity. However, they neglect that aerosolised pathogens can remain at a position where they were emitted after the infectious agent has gone. Thus, infection is possible without obvi-

\* simon.rahn@hm.edu

† marion.goedel@hm.edu

‡ gerta.koester@hm.edu

§ gesine.hofinger@team-hf.de

ous proximity.

Even if the infectious agent does not move, airflow may spread the pathogens and cause infections at distant places. Such transport mechanisms can be simulated with computational fluid dynamics (CFD) models. For example, Vuorinen et al. [11] simulate how the aerosols of a coughing person travel. However, CFD simulations require much, often uncertain information to set boundary conditions and, thus, to correctly capture a scenario. Even simple problems are computationally expensive. They become more demanding if CFD and crowd simulations are coupled, prohibiting scenarios with more than a few agents. Apart from that, the degree of detail between these two models does not match.

In summary, macroscopic compartmental models, agent-based models and CFD simulations allow analysing the spread of diseases on different scales. Macroscopic models consider the overall dynamics of an epidemic, whereas microscopic models focus on pathogen transmission between individuals. Gaining knowledge about the transmission on a local scale is of particular interest in the context of COVID-19. Small-scale proximity models neglect that pathogens may persist in aerosols, even if their source is no longer close. We wish to help bridge this gap and ask this question: How can we model airborne transmission of SARS-CoV-2 between individuals for everyday situations?

To answer this research question, we first introduce the methodology and our microscopic crowd model in Sec. II. In Sec. III, we formulate a mathematical model for pathogen transmission via aerosol clouds. We then computerise the model and couple it with crowd simulation in Sec. IV. We calibrate the parameters in Sec. V to match SARS-CoV-2. We also propose a reference scenario to which an agent’s degree of exposure in any other situation can be compared. Verification and validation in Sec. VI show that the model is implemented correctly and that its results reflect empirical data. In Sec. VII, we simulate a situation that is relevant for everyday life: transmissions between pedestrians waiting in a queue. Sec. VIII summarises and provides an outlook.

## II. METHODS AND MATERIALS

We adopt the classical modelling approach to build a new model for disease transmission. That is, we translate real-world observations into a mathematical formulation. Then, we implement this model as an algorithm and generate a calibrated simulation programme. This creates a virtual world in which we test various scenarios against empirical data. Verification and validation are essential steps to ensure that the software contains very few errors and that it yields results consistent with empirical observations. We validate our model by re-enacting two superspreading events.

The transmission model is integrated into Vadere [12], an established framework for microscopic crowd simula-

tion. We use the new sub-model in combination with the state-of-the-art Optimal Steps Model (OSM) [13, 14], but it is also compatible with other locomotion models. The source code and all relevant data are publicly available on Gitlab [15].

## III. MATHEMATICAL MODEL FOR TRANSMISSION VIA INHALATION

In this section, we model the transmission of SARS-CoV-2 among individuals via exhalation and inhalation. We develop our model specifically for COVID-19 but it can be transferred to other diseases that also spread through pathogens bound to aerosol particles, such as influenza [16]. As a first step, we operationalise real-world observations and derive a mathematical model.

### A. The agents’ state of health

Inspired by the compartmental SIR model [5], we define an agent’s health as susceptible (S), exposed (E), infectious (I) and recovered (R). **Susceptible** agents represent healthy persons. They inhale pathogens and accumulate them. Once the minimum infectious dose is exceeded, their status changes to exposed. **Exposed** agents are considered infected. They retain the attributes of susceptible agents but will become infectious after a latent period. This transition plays no role in our contribution since the time scale of our simulations ranges from minutes to a few hours, which is significantly shorter than the latent period for SARS-CoV-2. **Infectious** agents emit pathogens via aerosols. For simplicity, we do not distinguish between symptomatic and asymptomatic cases and keep the infectiousness constant. **Recovered** agents do not absorb pathogens, that is they are immune. Since the simulation time is short, they occur only if they are included in the initial condition of the simulation.

The cycle in Fig. 1 visualises the transition between health states, focussing on the transition from susceptibility to exposure.

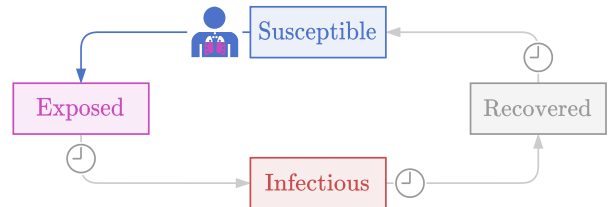


Figure 1: An agent’s health states: The transition from susceptible to exposed is relevant for the time scale of our model.

Independent of the current infection status, each agent

has a respiratory cycle of equally long periods of inhalation and exhalation. Pauses in between are neglected. Hence, we obtain the respiratory frequency  $f$  and the corresponding period  $T = f^{-1}$ . During exhalation, infectious agents emit pathogen bound to aerosol clouds. Susceptible agents inhale a fraction of these pathogens if their current position is within the aerosol cloud.

### B. Emission of pathogen

In the case of COVID-19, infectious persons emit pathogen mainly through aqueous droplets expelled during breathing, but also, e.g. by speaking or coughing. These expiratory events vary in intensity and, thus, in droplet numbers and droplet sizes [4], which in turn alters how the droplets spread through the air. Violent expiration causes larger droplets, which follow a ballistic trajectory, whereas normal breathing produces smaller droplets [4] that remain in the air and form a cloud around the source. In either case, there is a suspension of liquid particles in the air, which is often called aerosol. There is no clear line between small and large particles [17]. In this contribution, we consider particles that stay airborne for at least a few minutes. At this point, we focus on normal breathing. However, the concepts we present can be transferred to any kind of aerosol producing activity as long as the particles are small enough to stay airborne for some minutes.

An infectious agent creates an aerosol cloud containing pathogen particles with every exhalation. See Fig. 2.

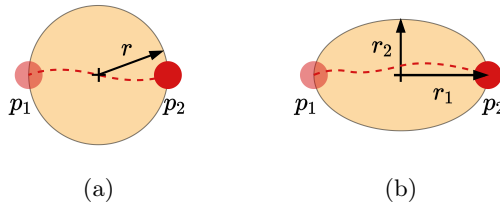


Figure 2: An infectious agent (red) emits aerosol clouds (orange). The shape of the cloud depends on the agent's speed. Low velocities lead to circular clouds (a) with radius  $r$ , whereas higher velocities yield elliptical clouds (b) with semi-axes  $r_1$  and  $r_2$ . The dashed line represents the agent's trajectory from left to right. The agent starts exhaling at  $p_1$  and stops at  $p_2$ .

We are aware that particle clouds can be very complex. However, we argue that modelling such detail would be unsuitable for the degree of abstraction of the overall model. Besides, airflow is often turbulent, making its computation a major and still unsolved problem. Hence, we decided to keep the model simple: since pedestrian dynamics are typically modelled in two dimensions, we represent each aerosol cloud by a two-dimensional shape in the horizontal layer. The initial cross-section  $A_0$  is equal for all clouds. In the case where the agent moves

slowly, the shape is a circle with a radius  $r$  (Fig. 2a). We let the cloud form over the entire period of exhalation  $T$ , so the shape is centred between the position, where the agent starts breathing out  $p_1$ , and the position, where it stops  $p_2$ . In a case where the agent walks faster,  $|v| > 2rT^{-1}$ , we obtain an ellipse with vertices at  $p_1$  and  $p_2$  (Fig. 2b), with the cloud growing longer as the agent walks faster.

The extent of aerosol clouds changes over time, in particular, in the presence of airflow. Again, we choose to focus on the simplest situation, with stagnant air, as can be found in confined spaces without ventilation. Such places are deemed particularly risky for SARS-CoV-2 transmission. Any agent  $i$  who walks through a cloud with velocity  $v_i$  disperses aerosol particles. To capture this scenario, we enlarge the clouds' radius by  $\Delta r(t) = \Delta t \sum_i |v_i(t)|$  at each time step  $t$ . Factor  $\Delta t$  is the length of a simulation step. It ensures that the dispersion model is independent of the user's choice for  $\Delta t$ . In the case of an elliptical cloud, we proportionally increase the semi-axes  $r_1$  and  $r_2$ .

In reality, aerosol clouds spread in three dimensions. In addition, we need a model of pathogen concentration in a volume that agents can breathe in. Since we are unaware of empirical evidence on the spread of the aerosolised pathogen in a stagnant air volume, we stick to a simple description: a homogeneous distribution. We represent the aerosol clouds with two-dimensional shapes in a horizontal layer at the height of the agents' heads. From there, we imagine them to extend to the same volume as a sphere with a radius  $r$ :  $V = \frac{4}{3}\pi r^3$ . Thus, we can measure the clouds' pathogen load as concentration  $C_p$  in particles per cubic metre, which decreases when the cloud extends. Furthermore, we assume that the concentration accumulates where clouds overlap. The initial pathogen load is equal for all aerosol clouds that are emitted by the same agent. This initial number of pathogens depends on the individual's infectiousness. The pathogens of an aerosol cloud are inactivated after some time. In addition, aerosol particles evaporate, rise to higher air levels, or sediment. We simplify these complex processes by assuming an exponential decay of the number of pathogens with a half-life  $T_a$ .

### C. Absorption of pathogen

While in the vicinity of one or more aerosol clouds, susceptible and exposed agents breathe in pathogens. Each agent absorbs the number of pathogen particles  $N_p$  contained in the tidal volume  $V_T$ . The tidal volume is the volume inhaled and exhaled with each breath [18]. From this follows  $N_p = C_p V_T (1 - E_p)$ . Masks reduce  $N_p$  by their effectiveness  $E_p$ .  $C_p$  is the sum of the pathogen concentrations of all aerosol clouds at the agents' position. We neglect that inhalation removes pathogens from the surroundings.

The number of pathogens accumulated by an agent de-

scribes its degree of exposure. The minimum infectious dose is the number of pathogens required for infection. In the model, it marks the transition from susceptible to exposed. Its calibration poses a challenge since, at present, there is no consensus on the right value for SARS-CoV-2. We will discuss this further in Sec. V.

#### IV. COMPUTERISED MODEL

Here, we combine the transmission model with the OSM [13, 14], a state-of-the-art locomotion model for pedestrian dynamics implemented in the open-source framework Vadere [12]. Vadere is well-established for crowd simulations, which is why we adhere to its software architecture when we define important requirements for a new feature: The code should be compatible with existing structures, modular so that the transmission model can easily be enabled or disabled for different locomotion models and flexible to allow for adaptations by other developers.

##### A. Embedding in Vadere

This section covers the embedding of the transmission model in Vadere. It gives insight into the software structure and how developers can enhance the model or implement additional features.

The transmission model is integrated into Vadere’s simulation loop, a while-loop that updates all elements, mainly sources, targets and agents’ positions, as long as the simulation is running (Fig. 3). The simulation loop calls the transmission model independently of other models, keeping the programme modular and flexible. In particular, this allows combining transmission with any Vadere’s locomotion model. Note that a user must select a locomotion model when running Vadere, whereas using the transmission model is optional.

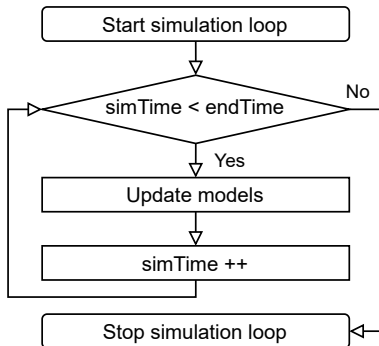


Figure 3: Models are updated as long as the simulation loop is running.

Fig. 4 visualises the structural embedding of the transmission model: The `TransmissionModel` implements the

interface `Model`, as the locomotion models in Vadere do. Supplementary features or alternative models for disease transmission can be added on the same level.

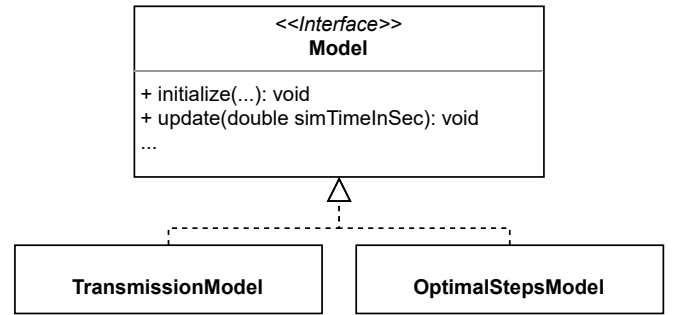


Figure 4: `TransmissionModel` contains the model core. Similar to the locomotion model `OptimalStepsModel`, it implements the interface `Model`.

`TransmissionModel`’s attributes contain general model parameters. Developers can adapt these attributes in the class `AttributesTransmissionModel`. We describe the meaning of each parameter in detail in Tab. I.

The methods of the class `TransmissionModel` contain most of the model’s logic. In essence, the method `update(...)` controls the emission of the pathogen and updates aerosol clouds and the agents’ health status. Each time an infectious agent stops exhaling, an aerosol cloud is inserted into the topography. Initially, the aerosol clouds cover the distance passed during the exhalation but can expand over time, whereas their pathogen load decreases exponentially. Aerosol clouds at the end of their lifetime are removed. Furthermore, the update method induces susceptible and exposed agents to absorb pathogens if they are in aerosol clouds. The routine also updates each agent’s respiratory cycle and infection status.

An agent’s health status is wrapped in the class `HealthStatus`, which is an attribute in `Pedestrian` as shown in Fig. 5. `HealthStatus` contains absorbed pathogen load, respiratory cycle and infection status as its most important attributes.

Aerosol clouds are embedded as `InfectiousParticleDispersion` that extends the class `ScenarioElement` and, thus, fit into the existing structure. Typical scenario elements are sources, targets or obstacles. This approach allows individual access and manipulation throughout the simulation runtime and facilitates the graphical representation of clouds.

##### B. Model parameters

In this section, we summarise all important model parameters. Users can adapt the values directly in the input file. The parameters apply to all agents and aerosol clouds within the same simulation. When an agent is

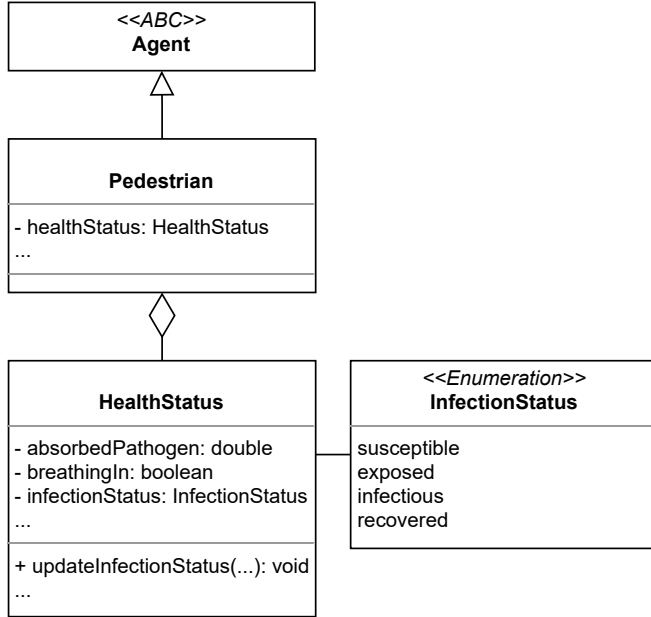


Figure 5: Pedestrians’ attributes wrapped in the class **HealthStatus**.

spawned, the parameter values are assigned to the agent’s attributes.

The agent’s health and aerosol clouds are partly defined by attributes listed in Tab. I. We are aware that, in reality, some parameters related to the agents’ health are time-dependent or differ from person to person. However, we do not expect significant changes within the simulation time, which is very short compared to the period of communicability. We capture the heterogeneity among infectious agents, e. g. pathogen load or position, by running separate simulations for adapted parameter sets.

## V. CALIBRATION

The model presented here allows simulating any disease transmitted by aerosols. We select a set of parameters to match the transmission of SARS-CoV-2 through aerosol clouds formed by normal breathing.

### A. Parameter set for SARS-CoV-2

The parameters are physical in the sense that we can directly transfer them from the real into the virtual world. Their values are summarised in Tab. I.

An adult at rest breathes approximately 12 to 18 times per minute. We use an average of 15 breaths per minute, which implies a period of  $T = 4\text{ s}$  between inhalations. The exact values depend on factors such as the level of physical activity. However, slightly different breathing rates affect the quantity of absorbed pathogens significantly less than other parameters. The emission capa-

city in particular, which describes the number of emitted pathogens per breath, may vary in orders of magnitude for SARS-CoV-2. Ma et al. [19] found that some individuals exhale up to 400,000 viral particles per minute. With 15 breaths per minute, this means more than  $10^4$  viruses per exhalation. Note that it is unclear if the pathogens were also emitted through larger droplets. COVID-19 positive cases may emit significantly fewer pathogens, e. g. when viral replication is low for their variant [20] or because they are not at the peak of their infectiousness. Since we are interested in observing infection spread, we simulate a highly infectious person with  $10^4$  particles per exhalation. To our knowledge, this represents the upper limit of a realistic range.

We now turn our attention to the absorbing, susceptible agents. The absorption rate  $R$  can be interpreted as the tidal volume in cubic metres. For an adult, it is approximately 0.5 litre, or  $R = 5 \cdot 10^{-4} \text{ m}^3$ , per inhalation. Masks would reduce this rate depending on their effectiveness.

The infectious dose  $D$  of SARS-CoV-2 in humans is still uncertain. It probably depends on the individual and the variant of the virus. Karimzadeh et al. [21] estimate that approximately  $10^2$  particles cause an infection. Popa et al. [22] analyse epidemiological clusters and infer that, on average, more than  $10^3$  viral particles can successfully start an infection, but smaller quantities may suffice. Since this parameter is uncertain, we re-examine it in section Sec. V B, where we calibrate the infectious dose through a reference scenario and set  $D = 3200$ .

The aerosol clouds are characterised by the following parameters: the initial area and the half-life. We assume an initial radius of  $r = 1.5 \text{ m}$  for circular aerosol clouds and, thus, an area of approximately  $A_0 = 7.1 \text{ m}^2$ . With the spheric extent described in Sec. III, we obtain a volume of  $V = 9.4 \text{ m}^3$ . Hence, the initial pathogen concentration of an aerosol cloud is about  $10^3$  particles per cubic metre. We rely on reports from experience for the half-life of an aerosol cloud’s SARS-CoV-2 load. The half-life of artificially generated aerosols was found to last from 30 min to several hours [23, 24]. The exact value for the half-life is not so important if the model output is interpreted qualitatively, as is the case in this contribution. However, it affects the dynamics of the model. A shorter half-life closely links exposure to the current location of an infectious agent. On the other hand, a long half-life means that agents can become exposed even if the infectious agent has left the area long ago.

### B. Calibration of the infectious dose

We gained parameter values on the transmission of SARS-CoV-2 from studies that have limitations. Therefore, we propose to evaluate simulation scenarios in relation to a reference: the so-called *close contact scenario*. We choose the number of pathogens that a susceptible agent absorbs in this situation as our infectious dose  $D$ .

Table I: Model parameters describing agents' health status and aerosol clouds. The values correspond to a highly infectious agent that exhales SARS-CoV-2.

Parameter	Symbol Description	Value	Unit
Agents' health status	<code>respiratoryCyclePeriod</code> $T$	Duration of one breath (inhalation and exhalation)	4 s
	<code>pathogenEmissionCapacity</code> $N$	Number of pathogen particles emitted per exhalation by an infectious agent; logarithmised to base 10	4 particles
	<code>pathogenAbsorptionRate</code> $R$	Relation of absorbed pathogens to the pathogens that are present in the surrounding; Interpretable as the agents' average tidal volume $V_T$ , potentially reduced by effectiveness $E_p$ of protective devices: $R = V_T (1 - E_p)$	$5 \cdot 10^{-4} \frac{\text{m}^3}{\text{inhalation}}$
	<code>minInfectiousDose</code> $D$	Number of pathogens required for an infection, that is, the $3.2 \cdot 10^3$ particles threshold above which an agent changes from susceptible to exposed	
Aerosol cloud	<code>initialArea</code> $A_0$	The cloud's extent at creation time; circular with radius $r$ and 7.1 elliptical with semi-axes $r_1$ and $r_2$ ; $A_0 = r^2 \pi = r_1 r_2 \pi$	$\text{m}^2$
	<code>halfLife</code> $T_a$	Defines the exponential decay of the pathogens in an aerosol cloud	600 s

Governmental and institutional instructions regarding contact tracing during the COVID-19 pandemic define close contacts as follows: A susceptible individual and a confirmed case of COVID-19 occupy an enclosed space without adequate ventilation. They are in close proximity for a certain time so that the susceptible person inhales aerosolised SARS-CoV-2 particles. The leading scientific institute in Germany in the context of the COVID-19 pandemic, Robert Koch Institute [25], declares a distance of less than 1.5 m for more than 10 min as critical. The Centers for Disease Control and Prevention, U.S. Department of Health and Human Services [26], specifies 6 ft  $\approx$  1.8 m for more than 15 min.

We follow the former definition with the parameter set from Tab. I. Two agents are placed less than 1.5 m apart (Fig. 6). Both remain stationary for 10 min.

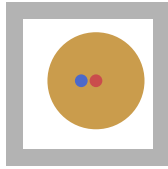
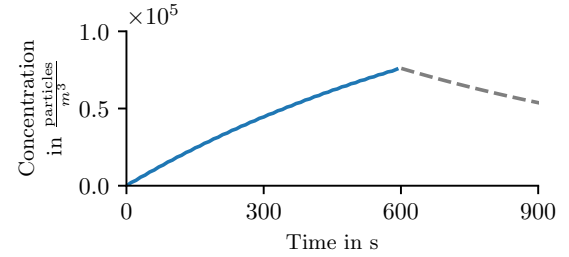


Figure 6: *Close contact scenario*: a highly infectious agent (red) emits pathogens bound to aerosols (orange) in an unventilated enclosed space. A susceptible agent (blue) absorbs pathogens.

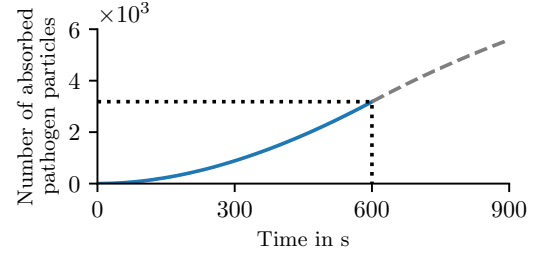
The infectious agent constantly emits aerosol clouds, thereby increasing the pathogen concentration. The susceptible agent absorbs approximately 3200 pathogen particles within 10 min (see Fig. 7). In all further simulations, agents who inhale  $D = 3200$  or more pathogens are considered exposed.

As soon as the infectious agent leaves the scenario, e. g. at  $t = 600$  s, the pathogen concentration decreases exponentially. If the susceptible agent remains, it will keep inhaling pathogen particles from the persistent aerosol

clouds (see Fig. 7).



(a) Pathogen concentration of aerosol clouds adds up.



(b) Pathogen load absorbed by the susceptible agent.

Figure 7: *Close contact scenario*: an infectious agent emits aerosol clouds so that the pathogen concentration builds up. The susceptible agent absorbs approximately 3200 particles within the critical period of 600 s (dotted lines). The dashed lines represent an extension of the scenario: The infectious agent leaves at  $t = 600$  s, whereas the susceptible agent remains and keeps absorbing pathogen from the exponentially decaying aerosol clouds.

## VI. VERIFICATION AND VALIDATION

Generally, careful verification and validation are necessary parts of the modelling and software development

processes. We verify the transmission model by running unit tests. The test coverage of the core of our model reaches approximately 80%. Vadere's continuous integration pipeline also contributes additionally to detecting errors in the code, as every commit is tested automatically. The locomotion models have been verified with unit tests and validated with standardised scenarios according to the Guideline for Microscopic Evacuation Analysis (RiMEA) [12].

The validation of the transmission model, however, poses a challenge since empirical studies on local infection spread, in particular related to SARS-CoV-2, are scarce. Fortunately, some data on superspreading events are available and are sufficiently detailed to be compared to simulations. Superspreading means that one or relatively few individuals infect numerous people [27]. Since it also plays a significant role in the transmission dynamics of SARS-CoV-2 [28], it becomes the core of our validation.

Majra et al. [29] presented an overview of recorded events. Unfortunately, only a few situations can be simulated with our model, and even fewer are suitable for validation. Firstly, the model is designed to capture the transmission via aerosol clouds mostly stagnant for at least several minutes. Thus, strong flows should not dominate the air circulation at the event. Secondly, the event must not be too complex to be meaningfully represented in a simulation scenario. For example, the unknown routes of hundreds of guests at a carnival party would have to be guessed, making any comparison of data doubtful.

We find that the following events fit our purpose best: SARS-CoV-2 spread in a restaurant with ten infected people [30] and during a choir rehearsal, where 52 of 61 attendees became infected [2, 31]. Both events occurred and were investigated in the early phase of the pandemic when science and society were still relatively unaware of SARS-CoV-2. Consequently, other than the more recent events, measures such as physical distancing, air filtering or masks were absent. These would introduce further complexity because they must be adequately modelled and validated. We avoid this for the validation reported here. Effects of these measures can be introduced into the model by adapting the values of parameters, e. g. particles exhaled or half-life of the aerosol cloud. The reports provide information about the number of secondary cases, that is infected persons but not about the individual number of absorbed particles. We solve this by assuming that an agent is exposed if it inhales the same amount of pathogen as in the reference scenario, that is, 3200 virus particles. We will also compare to a dose of 1000, as suggested in the literature. The parameter settings for the locomotion model for both validation cases are listed in the appendix (Tab. III).

We start with the spreading event in a restaurant in January 2020: Ten persons, divided into groups A, B and C, were sitting at adjacent tables. The infectious index patient belonged to group A. Group A shared the

restaurant with group B for 53 min and with group C for 73 min. All ten individuals were tested positive after the restaurant visit. It was determined that the index case infected at least one member of groups B and C while in the restaurant. Further transmission among each group in the following days is considered possible. The topography is shown in Fig. 8.

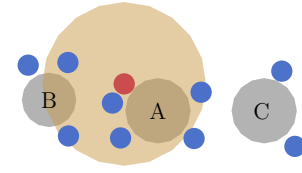


Figure 8: Model of restaurant topography, including tables and seats, according to the seating chart in [30].

Susceptible (blue) agents sit in groups A, B and C around the tables (grey). The infectious (red) agent emits aerosol clouds (orange).

We consider our simulation as qualitatively valid if we observe infection spread below the numbers in the study. We argue that the simulation ignores airflow between tables from the restaurant's ventilation as well as any transmission after the event. In the simulation, five agents become exposed, and among them, three from group A, two from group B and none from group C, that is, half the number of the true cases.

The choir rehearsal in March 2020 is significantly more complex: 1 of 61 attendees was symptomatic. After the practice, 33 people, including the index patient, were tested positive. Twenty further attendees are considered probable cases because they became ill but were not tested. One person, initially classified as a probable case, tested negative after the onset of symptoms. Thus, we use a minimum of 32 and a maximum of 52 secondary cases as reference values to which we compare our simulation results.

Again, we expect fewer exposed agents in our simulation than in reality. In addition, we do not have sufficient information about close interactions between the attendees during arrival and departure to include them in the simulation. As a consequence, we ignore opportunities for droplet transmission. Moreover, singing forcibly propels droplets, increasing pathogen spread.

The choir practice occurred in a large room and, partly, in a smaller room. The attendees changed their positions from time to time, which we model by allowing the agents to move from one intermediate target to another. The study did not provide a seating chart citing privacy concerns. Thus, we imitate the seating arrangement from [2] qualitatively but must make assumptions about the floor plan: Fig. 9. The rooms cover an area of approximately  $28 \text{ m} \times 12 \text{ m}$ . Smaller intermediate targets (orange) mark possible seating positions during the practice sessions.

Miller et al. [2] report the following schedule: During the first  $T_1 = 45 \text{ min}$ , all choir members practised

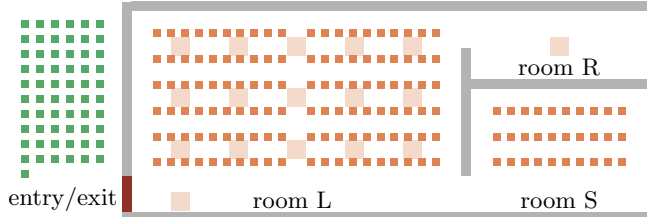


Figure 9: Choir practice topography: a large (L) hall, a small (S) room and a restroom (R). Agents are spawned by sources (green), they approach an intermediate target, remain there for a given period and move to the next one (targets all orange). Small orange squares represent chairs. Large, light orange squares define positions where agents gather in small groups during the break. The agents exit the scenario through the red door.

together in the large room L. Some seats between individuals were empty. A 45-min ( $T_2$ ) sectional rehearsal followed during which the attendees were divided into two groups, one in room L, the other in room S. The index case remained in room L. After that, there was a break of approximately  $T_3 = 10$  min. This allowed for mingling, and a few people, including the index case, used the restroom. The positions during the break are not reported. We assume that the choir members gathered in small groups distributed across room L. For the last session of  $T_4 = 50$  min, everybody returned to their original positions in room L.

We simplify the schedule. Firstly, we choose practice sessions of equal length ( $T_1 = T_2 = T_4 = 45$  min), which makes the definition of intermediate target positions in the simulation easier. Secondly, we ignore the fact that the attendees arranged chairs before and after the rehearsal, arguing that the time for this appears short compared to the entire practice. While these two aspects may be negligible, we acknowledge that the attendees' exact positions in space and time would be essential. They would reveal where high pathogen concentrations can occur and, where exposure is likely. Unfortunately, this information was not recorded and must remain uncertain.

We deal with this by applying Monte Carlo techniques: We evaluate the model  $M = 100$  times, collect the simulation output and summarise it statistically. The simulations differ only in the agents' paths. We achieve this by randomly mapping the agents to their intermediate targets for each simulation set-up. Fig. 10 shows a histogram of the simulation output, that is, the number of exposed agents. As discussed in Sec. IV B, the infectious dose is uncertain and may depend on individuals' immune systems. A dose of  $D = 3200$  pathogen particles corresponds to the close contact scenario, whereas  $D = 1000$  was estimated in [22].

We observe that the simulation results for both parameter choices are of the order of magnitude that was reported for the real event, but with fewer exposed agents.

This is what we expected and regarded the simulation result as proof of our model's validity.

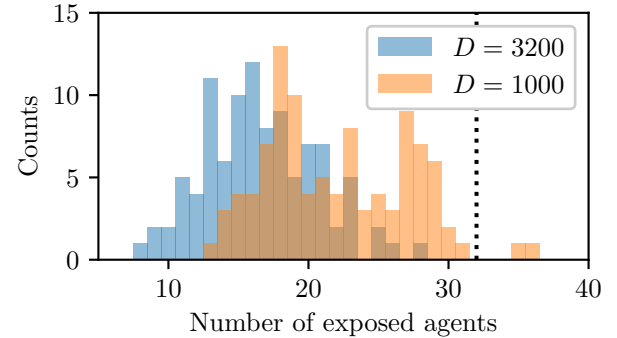


Figure 10: Number of exposed agents for  $M = 100$  simulations. Blue: infectious dose of  $D = 3200$  pathogen particles. Orange: a more vulnerable population with  $D = 1000$ . The dotted line indicates the 32 confirmed secondary cases of the true spreading event.

## VII. APPLICATION TO A QUEUE SCENARIO

In this section, we use the transmission model to evaluate exposure in a queue in front of a service unit, e.g. a counter at a shopping centre, a cinema, an office or any other similar situation. We simulate one highly infectious person among several susceptible pedestrians. In the green area, one source spawns nine susceptible agents, and a second source spawns a single infectious agent at the fifth position. Belt barriers guide the meandering queue to the counter, where each agent is served for a fixed time  $T_s = 120$  s. The agents immediately leave the topography as soon as they pass the counter. The topography, as shown in Fig. 11, may represent a part of a building, covering an area of  $5\text{ m} \times 7\text{ m}$ . In terms of validation scenarios, the parameter settings for the locomotion model are listed in Tab. III of the appendix, allowing third parties to repeat and check our computer experiment.

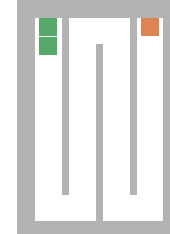


Figure 11: Queue topography: agents (blue) start at the source (green) and move towards the service unit (orange). Belt barriers are shown as grey obstacles.

Fig. 12 shows the queue for several time steps. The colour, ranging from blue (susceptible) to violet (exposed),

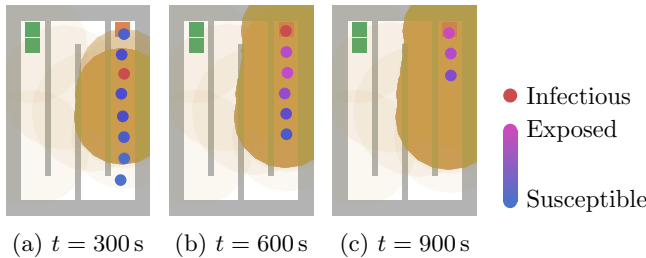


Figure 12: Susceptible agents (blue) are exposed to pathogens in aerosol clouds (orange circles) exhaled by an infectious agent (red). The opacity of aerosol clouds reflects their current pathogen concentrations. The agents’ colour change, from blue to violet, indicates their degree of exposure.

indicates the number of pathogens accumulated in an agent. All aerosol clouds remain at their initial positions because we assume stable air layers. Hence, high concentrations occur where many clouds are superimposed.

This pathogen concentration visualisation aids us in identifying potentially risky situations. The sixth, seventh and eighth positions in this queue, behind the infectious agent, are critical, as agents directly step into and remain in the recently contaminated area. The agents at these positions absorb more than  $D = 3200$  pathogen particles, that is, they carry at least the same infection risk as the close contact in the reference scenario. However, the seventh and eighth positions are not a close contact position. The infectious agent queues for 10 min. The seventh and eighth agent are within 1.5 m of the infectious agent for less than half of this time and continue to inhale contaminated air after the infectious agent has left.

Our simulation supports the claim that queues, in stagnant air, pose a severe infection risk. However, how could the risk of exposure be reduced? We propose to evaluate measures by varying the model parameters that reflect these measures. For example, a mask worn by the infectious agent would reduce the number of pathogens. In addition, social distancing could be introduced. Organisers could strive to avoid this type of queue, e.g. by handing out service numbers, or they could install overhead ventilation.

## VIII. CONCLUSION AND OUTLOOK

We complemented microscopic crowd simulation with a new model for the transmission of pathogens via small aerosol particles within Vadere, an open-source framework for simulating pedestrian dynamics. Infectious agents exhale pathogens bound to aerosol clouds, whereas susceptible individuals absorb pathogens. We calibrated parameters to the transmission of SARS-CoV-2 and re-enacted two superspreading events for which we obtained

qualitatively plausible results.

As a result, we demonstrated how to evaluate the risk of exposure in everyday situations using our simulation model: we observed the number of pathogen particles absorbed by agents in a typical queue. We compared the result to a reference value obtained from a benchmark scenario: a close contact situation acknowledged as high risk in the context of SARS-CoV-2 by official health authorities. As long as there is no consensus on the true infectious dose for SARS-CoV-2, we propose interpreting agents as exposed if they inhale as many viruses as in the reference scenario.

As a next step, we plan to refine the temporal and spatial spread of aerosols in the model. In addition, we propose analysing additional scenarios, including the variation of parameters, to evaluate the effectiveness of measures, to account for immunisation as well as an evolving virus. Beyond that, we hope that our model will be adapted, when the need arises, by other scientists to investigate future pandemics.

## ACKNOWLEDGEMENT

We thank Dr Mareike Mähler, Dr Laura Künzer, Dr Désirée Dahmen, and Nele Clemen (Team HF) for support with literature research related to the COVID-19 pandemic. We thank Dr Angelika Kneidl (accu:rate GmbH) and Prof. Dr Christian Schwarzbauer (Munich University of Applied Sciences HM) for valuable discussions and Dr Andreas Wieser (Ludwig Maximilian University of Munich) for information about the infectiousness of COVID-19 patients.

*a. Authors’ contributions* Conceptualisation S. R., M. G. and G. K.; Data curation S. R.; Formal analysis S. R. and M. G.; Funding acquisition G. K.; Investigation S. R. and G. H.; Methodology S. R. and M. G.; Project administration G. K.; Resources G. K.; Software S. R.; Supervision G. K.; Validation S. R.; Visualization S. R.; Writing – original draft S. R.; Writing – review & editing M. G., G. K. and G. H.. All authors gave final approval for publication and agree to be held accountable for the work performed therein.

*b. Funding* S. R., M. G., G. K., and G. H. are supported by the German Federal Ministry of Education and Research through the project CovidSim (grant no. 13N15662).

*c. Competing interest* The authors declare that there is no conflict of interest.

*d. Data accessibility* The datasets supporting this article have been uploaded to [15].

[1] World Health Organization. Who Director-General's opening remarks at the mediabriefing on COVID-19 - 11 March 2020, 2020. <https://www.who.int/director-general/speeches/detail/who-director-general-s-opening-remarks-at-the-media-briefing-on-covid-19---11-march-2020>. Accessed on November 8, 2021.

[2] S. L. Miller, W. W. Nazaroff, J. L. Jimenez, A. Boerstra, G. Buonanno, S. J. Dancer, J. Kurnitski, L. C. Marr, L. Morawska, and C. Noakes. Transmission of SARS-CoV-2 by inhalation of respiratory aerosol in the skagit valley chorale superspreading event. *Indoor Air*, 31(2): 314–323, 2020. doi:10.1111/ina.12751.

[3] L. Zhou, S. K. Ayeh, V. Chidambaram, and P. C. Karakousis. Modes of transmission of SARS-CoV-2 and evidence for preventive behavioral interventions. *BMC Infectious Diseases*, 21(1), 2021. doi:10.1186/s12879-021-06222-4.

[4] Gesellschaft Für Aerosolforschung e.V. Position paper of the Gesellschaft für Aerosolforschung on understanding the role of aerosol particles in SARS-CoV-2 infection. 2020. doi:10.5281/zenodo.4350494.

[5] W. O. Kermack and A. G. McKendrick. A contribution to the mathematical theory of epidemics. *Proceedings of the Royal Society of London. Series A, Containing Papers of a Mathematical and Physical Character*, 115(772):700–721, 1927. doi:10.1098/rspa.1927.0118.

[6] M. Abadeer and S. Gorlatch. Simulating infection transmission: A case study of COVID-19. pages 310–317, 2020. URL <https://www.scopus.com/inward/record.uri?eid=2-s2.0-85096745031&partnerID=40&md5=fd5dee05ef393a85cd40b5d42e55ef4>.

[7] L. Goscé, D. Barton, and A. Johansson. Analytical modelling of the spread of disease in confined and crowded spaces. *Scientific Reports*, 4(1), 2014. doi: 10.1038/srep04856.

[8] A. Johansson and L. Goscé. Utilizing crowd insights to refine disease-spreading models. In *Pedestrian and Evacuation Dynamics 2012*, pages 1395–1403. Springer International Publishing, 2013. doi:10.1007/978-3-319-02447-9\_116.

[9] S. Namilae, P. Derjany, D. Liu, A. Mubayi, and A. Srinivasan. Multiscale pedestrian dynamics and infection spread model for policy analysis. volume 5, pages 512–514. Forschungszentrum Jülich, Zentralbibliothek, 2020. doi:10.17815/cd.2020.86.

[10] E. Ronchi and R. Lovreglio. Exposed: An occupant exposure model for confined spaces to retrofit crowd models during a pandemic. *Safety Science*, 130(104834), 2020. doi:10.1016/j.ssci.2020.104834.

[11] V. Vuorinen, M. Aarnio, M. Alava, V. Alopaeus, N. Atanasova, M. Auvinen, N. Balasubramanian, H. Bordan, P. Eröstö, R. Grande, et al. Modelling aerosol transport and virus exposure with numerical simulations in relation to SARS-CoV-2 transmission by inhalation indoors. *Safety Science*, 130:104866. ISSN 0925-7535. doi:10.1016/j.ssci.2020.104866.

[12] B. Kleinmeier, B. Zönnchen, M. Gödel, and G. Köster. Vadere: An open-source simulation framework to promote interdisciplinary understanding. *Collective Dynamics*, 4, 2019. doi:10.17815/CD.2019.21.

[13] M. J. Seitz and G. Köster. Natural discretization of pedestrian movement in continuous space. *Physical Review E*, 86(4):046108, 2012. doi:10.1103/PhysRevE.86.046108.

[14] I. von Sivers and G. Köster. Dynamic stride length adaptation according to utility and personal space. *Transportation Research Part B: Methodological*, 74: 104–117, 2015. doi:10.1016/j.trb.2015.01.009.

[15] Vadere: Open source framework for pedestrian simulation. Available online: <https://gitlab:1rz:de/vadere/-/commit/095ed1242aa1ca9867bf7c970c7897fdf016bd94>, 2021. Commit: 095ed124.

[16] R. Tellier. Aerosol transmission of influenza A virus: a review of new studies. *Journal of The Royal Society Interface*, 6:S783–S790, 2009. doi: 10.1098/rsif.2009.0302.focus.

[17] Umweltbundesamt. Infektiöse Aerosole in Innenräumen, 2021. Available online: <https://www.umweltbundesamt.de/themen/gesundheit/umwelteinflusse-auf-den-menschen/innenraumluft/infektioese-aerosole-innenraeumen#was-sind-aerosole->. Accessed on: 17 March 2021.

[18] M. F. Lutfi. The physiological basis and clinical significance of lung volume measurements. *Multidiscip Respir Med.*, 12(1). doi:10.1186/s40248-017-0084-5.

[19] J. Ma, X. Qi, H. Chen, X. Li, Z. Zhang, H. Wang, L. Sun, L. Zhang, J. Guo, L. Morawska, et al. Coronavirus disease 2019 patients in earlier stages exhaled millions of severe acute respiratory syndrome coronavirus 2 per hour. *Clinical Infectious Diseases*, 72(10):e652–e654, 2020. doi:10.1093/cid/ciaa1283.

[20] P. Mlcochova, S. A. Kemp, M. S. Dhar, G. Papa, B. Meng, I. A. T. M. Ferreira, R. Datir, D. A. Collier, A. Albecka, S. Singh, et al. SARS-CoV-2 b.1.617.2 delta variant replication and immune evasion. *Nature*, 599(7883):114–119, 2021. doi:10.1038/s41586-021-03944-y.

[21] S. Karimzadeh, R. Bhopal, and H. N. Tien. Review of infective dose, routes of transmission and outcome of COVID-19 caused by the SARS-CoV-2: comparison with other respiratory viruses— CORRIGENDUM. *Epidemiology and Infection*, 149:e116, 2021. doi: 10.1017/s0950268821001084.

[22] A. Popa, J.-W. Genger, M. D. Nicholson, T. Penz, D. Schmid, S. W. Aberle, B. Agerer, A. Lercher, L. Endler, H. Colaço, et al. Genomic epidemiology of superspreading events in austria reveals mutational dynamics and transmission properties of SARS-CoV-2. *Science Translational Medicine*, 12(573):eabe2555. doi: 10.1126/scitranslmed.abe2555.

[23] N. van Doremalen, T. Bushmaker, D. H. Morris, A. Gamble, B. N. Williamson, A. Tamin, J. L. Harcourt, N. J. Thornburg, S. I. Gerber, J. O. Lloyd-Smith, et al. Aerosol and surface stability of SARS-CoV-2 as compared with SARS-CoV-1. *New England Journal of Medicine*, 382(16):1564–1567, 2020. doi: 10.1056/NEJMc2004973.

[24] S. J. Smither, L. S. Eastaugh, J. S. Findlay, and M. S. Lever. Experimental aerosol survival of SARS-CoV-2 in artificial saliva and tissue culture media at medium and

high humidity. *Emerging Microbes & Infections*, 9(1):1415–1417, 2020. doi:10.1080/22221751.2020.1777906.

[25] Robert-Koch-Institut. Kontaktpersonen-Nachverfolgung bei SARS-CoV-2-Infektionen, Stand 11.8.2021. Available online: [https://www.rki.de/DE/Content/InfAZ/N/Neuartiges\\_Coronavirus/KontaktpersonenManagement.html](https://www.rki.de/DE/Content/InfAZ/N/Neuartiges_Coronavirus/KontaktpersonenManagement.html). Accessed on: 8 November 2021.

[26] Centers for Disease Control and Prevention. Scientific brief: SARS-CoV-2 transmission. Available online: <https://www.cdc.gov/coronavirus/2019-ncov/science/science-briefs/sars-cov-2-transmission.html>. Accessed on: 8 November 2021.

[27] D. Lewis. Superspreading drives the COVID pandemic — and could help to tame it. *Nature*, 590(7847):544–546, 2021. doi:10.1038/d41586-021-00460-x.

[28] B. M. Althouse, E. A. Wenger, J. C. Miller, S. V. Scarpino, A. Allard, L. Hébert-Dufresne, and H. Hu. Superspreading events in the transmission dynamics of SARS-CoV-2: Opportunities for interventions and control. *PLOS Biology*, 18(11):e3000897, 2020. doi:10.1371/journal.pbio.3000897.

[29] D. Majra, J. Benson, J. Pitts, and J. Stebbing. SARS-CoV-2 (COVID-19) superspreader events. *Journal of Infection*, 82(1):36–40, 2021. doi:10.1016/j.jinf.2020.11.021.

[30] J. Lu, J. Gu, K. Li, C. Xu, W. Su, Z. Lai, D. Zhou, C. Yu, B. Xu, and Z. Yang. COVID-19 outbreak associated with air conditioning in restaurant, guangzhou, china, 2020. *Emerging Infectious Diseases*, 26(7):1628–1631, 2020. doi:10.3201/eid2607.200764.

[31] L. Hamner, P. Dubbel, I. Capron, A. Ross, A. Jordan, J. Lee, J. Lynn, A. Ball, S. Narwal, S. Russell, et al. High SARS-CoV-2 attack rate following exposure at a choir practice — skagit county, washington, march 2020. *MMWR. Morbidity and Mortality Weekly Report*, 69(19):606–610, 2020. doi:10.15585/mmwr.mm6919e6.

## Appendix A: Detailed parameter set-up

To allow third parties to replicate our computer experiment, we provide more detailed information about the model set-up. In principle, all scenario files can be accessed on Gitlab [15]. However, the following parameter sets should be used to reproduce the simulations independently: All (pseudo-)random numbers used in the simulations with Vadere can be generated with the seeds listed in Tab. II.

Table II: Simulation parameters.

Scenario	fixedSeed
Close contact	8838372581797678424
Restaurant	4889043484410943750
Choir rehearsal	–2054058476485033808
Queue	1436250873317888407

We also adapted the parameters of Vadere for the OSM to fit the agents' locomotion behaviour to the simulated situation. The modifications to the default settings are listed in Tab. III. The scenarios used for the validation require minor adaptations to the pedestrians' potential. These affect the distance between an agent and other agents or obstacles. For the queue scenario, we enabled a greater sensitivity regarding thin obstacles (belt barriers). We also reduced the agents' attraction towards their target (counter) to reach more realistic distances between the agents in the queue.

Table III: Parameters of the Optimal Steps Model defining the agents' locomotion behaviour.

Scenario	seeSmallWalls	pedPotentialHeight	obstPotentialWidth	targetAttractionStrength
Default/close contact	false	50	0.8	1
Restaurant		5	0	
Choir rehearsal		5		
Queue	true			0.4